



Article

# 2D Positioning Control System for the Planar Motion of a Nanopositioning Platform

Lucía Díaz-Pérez <sup>1,\*</sup>, Marta Torralba <sup>2</sup>, José Antonio Albajez <sup>1</sup> and José Antonio Yagüe-Fabra <sup>1</sup>

<sup>1</sup> I3A—Universidad de Zaragoza, C/María de Luna, 3, 50018 Zaragoza, Spain; jalbajez@unizar.es (J.A.A.); jyague@unizar.es (J.A.Y.-F.)

<sup>2</sup> Centro Universitario de la Defensa Zaragoza, Ctra. Huesca s/n, 50090 Zaragoza, Spain; martatg@unizar.es

\* Correspondence: lcdiaz@unizar.es

Received: 24 October 2019; Accepted: 8 November 2019; Published: 13 November 2019



**Abstract:** A novel nanopositioning platform (referred as NanoPla) in development has been designed to achieve nanometre resolution in a large working range of 50 mm × 50 mm. Two-dimensional (2D) movement is performed by four custom-made Halbach linear motors, and a 2D laser system provides positioning feedback, while the moving part of the platform is levitating and unguided. For control hardware, this work proposes the use of a commercial generic solution, in contrast to other systems where the control hardware and software are specifically designed for that purpose. In a previous paper based on this research, the control system of one linear motor implemented in selected commercial hardware was presented. In this study, the developed control system is extended to the four motors of the nanopositioning platform to generate 2D planar movement in the whole working range of the nanopositioning platform. In addition, the positioning uncertainty of the control system is assessed. The obtained results satisfy the working requirements of the NanoPla, achieving a positioning uncertainty of ±0.5 µm along the whole working range.

**Keywords:** 2D positioning control; nanopositioning; Halbach linear motors; positioning uncertainty

## 1. Introduction

In recent years, the applications of nanotechnology and nanoscience have increased, demanding high accuracy positioning systems capable of working in large ranges at the nanometre scale. These positioning stages can be used for measuring or nanomanufacturing applications by integrating different devices [1]. The performance of these processes is directly related to the accuracy of the positioning systems and their working range [2]. Therefore, accurate positioning control in a large working range is one of the main necessities of nanotechnology applications [3].

At the University of Zaragoza, a novel 2D nanopositioning platform (NanoPla) is in development [4]. This NanoPla has been designed to work together with different kinds of tools and probes in various applications, such as metrology or nanomanufacturing. In particular, the main application of this first prototype is surface topography characterisation at the atomic scale of samples with relatively large planar areas. The measuring device will be attached to a moving platform that performs a large displacement of 50 mm × 50 mm. The NanoPla architecture is based on a scheme of the four integrated custom-made Halbach linear motors, which allow the implementation of planar motion [5]. The XY position of the platform is measured by a 2D plane mirror laser interferometer system. The design of the NanoPla has been optimised to achieve a nanometre resolution along its whole working range [6].

A commercial control solution for these custom-made linear motors is not currently available. Thus, in other previous works [7,8], control hardware and software were specifically designed and

built for control issues. In contrast, in this project, the use of commercial control hardware for generic motors has been proposed as a novel solution for their control and drive systems. The purpose of this research is to facilitate the future replicability of the system. In a previous study [9], a 1D positioning control strategy was designed and implemented in the selected commercial control hardware for one linear motor performing movement on a linear guide. The right performance of this control system, according to the established design requirements, was experimentally verified. In this work, the control strategy is optimised for 2D movement and implemented in the NanoPla to control and drive the planar motion of a nanopositioning platform in a range of 50 mm × 50 mm. Subsequently, the positioning uncertainty of the proposed control system is analysed.

This article is an extension of the work presented in a previous conference paper [10] and is divided as follows. Firstly, an overview of the NanoPla is presented, and the Halbach linear motors, the positioning sensor, and the hardware of the control system are described. Secondly, a positioning 2D control system is proposed and experimentally validated. Then, the positioning uncertainty of the 2D positioning control system is assessed. Finally, conclusions are developed.

## 2. Materials and Methods

This section describes the NanoPla's design and its applications. Additionally, the control system's hardware is defined, as well as the actuators, the positioning sensor, and the connections between them.

### 2.1. 2D Nano-Positioning Platform (NanoPla)

The NanoPla design was presented in [6]. An exploded view of the NanoPla can be seen in Figure 1. This platform has a three-layered structure that consists of fixed inferior and superior bases and a moving platform that is placed between them. The metrology loop consists of two metrology frames: One in the moving platform (I) and the other in the inferior base (II). The structural parts of the NanoPla are made of the aluminium alloy 7075-T6 due to its strength, which is comparable to many steels. In this first prototype for preliminary tests, the metrology frame is made of the same aluminium. Nevertheless, the selected material for its final design is Zerodur, due to its low thermal expansion coefficient that assures negligible dimensional changes caused by temperature variation.

The moving platform is levitated by three vacuum-preloaded air bearings, while four Halbach linear motors perform its motion. A Halbach linear motor has two parts: A permanent magnet array and a stator that consists of three-phase ironless coils. In the NanoPla, the magnet arrays of the four linear motors are fixed to the moving platform, and the stators are assembled to the superior base, which minimises the weight of the moving part. A 2D laser interferometer system works as a positioning sensor. The laser heads are positioned in the inferior base, and the positioning mirrors are fixed to the moving platform. Out-of-plane deviations are characterised by three capacitive sensors. As a probe, the aim is to embed an atomic force microscope (AFM) in the NanoPla. The AFM is fixed to the moving platform that positions it in the XY-plane above the certain area of the sample to be measured, allowing the characterization of a large area of the sample (50 mm × 50 mm). Once the AFM is positioned, the moving platform remains static (air bearings off) in order to carry out the scanning task.

The NanoPla offers a two-stage scheme, that is, the XY-long range positioning of the moving platform (coarse motion) is complemented by an additional piezo-nanopositioning stage that is fixed to the metrology frame of the inferior base (fine motion). This second stage is a commercial piezo-nanopositioning device specifically designed for the scanning probe and optical microscopy (model NPXY100Z10A from nPoint). It has a XYZ working range of 100 µm × 100 µm × 10 µm and a positioning noise of 0.5 nm in the XY-plane and 0.1 nm in Z-axis. During the scanning operation, the piezostage will perform the motion of the sample. Therefore, the position control system should have a positioning error at least one order of magnitude smaller than the maximum XY range of the commercial piezo-nanopositioning stage (i.e., 10 µm). Thus, this error could be corrected by the fine motion of the piezo stage.

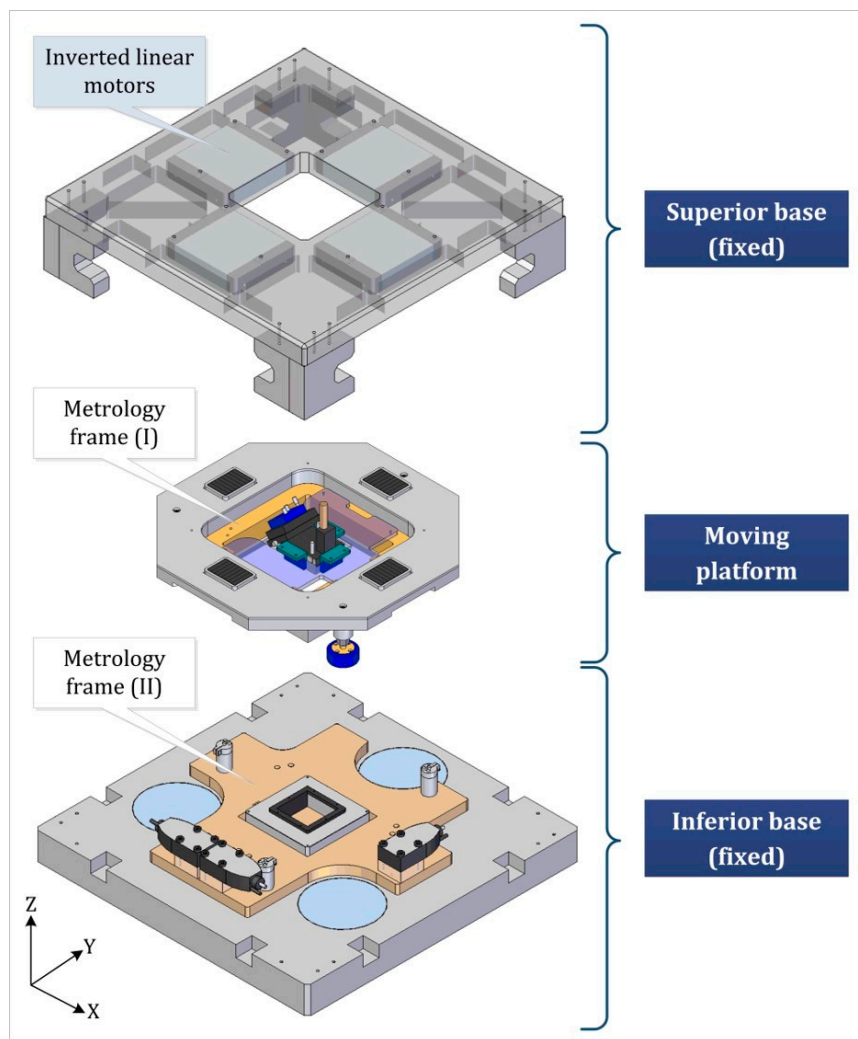


**Figure 1.** Exploded view of the nanopositioning platform (NanoPla).

## 2.2. Components of the Control System

The positioning systems' main components are actuators, control hardware, and positioning sensors. The selection of these components is based on the positioning stage's required precision, as well as the operating range and structure of the stage. Similarly, the development of the control strategy is constrained by the positioning system components defined by the NanoPla's design. In addition, the implementation of the components in the positioning control system can be optimised to leverage the capabilities of each of component in order to obtain the maximum positioning accuracy.

Halbach linear motors directly transform electrical energy into linear motion and have been selected as actuators in the NanoPla because of their many advantages in precision engineering due to their lack of mechanical transmission elements (thereby avoiding, for example, backlash). Similarly, contactless unguided motion prevents friction and allows planar motion. Planar motion is preferred in precision applications because it minimises geometrical errors and presents many other advantages in precision engineering [11]. The Halbach linear motors used in the NanoPla were developed by Trumper et al. [5] and are not commercialised. Therefore, they have been custom-made at the University of North Carolina at Charlotte, and the size of their winding areas is large enough to allow planar movement in the 2D working range of the NanoPla. When DC current flows through the three-phase coils of a Halbach linear motor, the electric field interacts with the magnetic field of the magnet array, resulting in two orthogonal forces—one horizontal and the other vertical. The relationship between

the phase currents and the generated forces is defined by the motor law presented in [9]. The vertical forces of the four motors facilitate the moving platform's levitation, while the horizontal forces move the platform in the XY-plane.

A generic commercial control system for custom-made Halbach linear motors is not currently available. For this reason, other reviewed stages integrating these motors specifically designed and developed control hardware and software for this purpose [7,8]. In these stages, control strategies are based on individually and independently controlling each of the phase currents of the motors with transconductance power amplifiers. However, following the NanoPla's design principle of integrating commercial devices when possible, the use of only commercial hardware and no custom-made electronics was proposed. Thus, a Digital Motor Control Kit (DMC) DRV8302-HC-C2-KIT from Texas Instruments was selected as the control hardware. The DMC kit consists of a F28035 control card and a DRV8302 board. This DMC kit has been designed for rotary brushless DC and permanent magnet synchronous three-phase motors, where the aim is to control the rotation speed or the torque generated. The board includes a three-phase power stage that drives and generates phase voltages by pulse-width modulation (PWM), in contrast to other works [7,8] where the hardware acted as a controlled current source. Additionally, the control hardware forces the star connection of the phases, thereby impeding the phase currents from being controlled independently, as was done in [7,8]. This hardware has been selected due to its relatively low cost and the advantages of the associated software. The use of the microcontroller from Texas Instruments is based on the Target Support Package™ for Embedded Code. This Package integrates MATLAB® and Simulink® with Texas Instrument tools and C2000 processors to generate, compile, implement, and execute the optimised control code with a user-friendly graphic interface and without programming in a specific language.

As mentioned, in the NanoPla, a 2D laser system is used as a positioning sensor to provide control system feedback. This 2D laser system is a combination of three 1D plane mirror laser interferometer systems. Laser interferometer systems provide highly accurate, non-contact measurements and are capable of working at long distances [12]. In addition, the use of plane mirrors as retroreflectors allows one to measure planar motion [13]. Two laser beams are needed to measure the displacement in the X- and Y-axes. In addition, one more beam is needed to determine the rotation around Z-axis. Thus, one laser head is placed projecting its beam in the X-axis, aligned with the reference system of the travel range, while the other two laser heads project their beams parallel to the Y-axis. The laser system components belong to the Renishaw RLE10 laser interferometer family, which consists of a laser unit (RLU), three sensor heads (RLD), two plane mirrors (one per axis), and an environmental control unit (RCU). Furthermore, an external interpolator is used to reduce the expected resolution of the system from 9.88 nm to 1.58 nm. Besides the readouts of the three laser encoders, the system also provides the readouts of the RCU sensors: Air temperature, material temperature, and air pressure. The measurement of each signal takes approximately 0.04 s; thus, the maximum speed at which it is possible to record the six measurements is every 0.25 s.

In a previous work [9], an experimental setup, external to the NanoPla, was assembled for the development and experimental validation of the control system of one Halbach linear motor in 1D. In that setup, the magnet array of the motor was fixed, and the stator of the motor was the moving part, attached to a pneumatic linear guide. A control strategy was implemented in the DMC kit, and a 1D interferometer laser system was used as the positioning sensor. After that first validation, the four linear motors were installed in the NanoPla, and each of them connected to one DMC Kit for the project presented in this paper. In turn, all the DMC kits were connected to the host PC that coordinated the four motors. Movement was achieved while the moving platform was levitated by three air bearings. Figure 2a is a photograph of the NanoPla and the control system components, while Figure 2b illustrates a scheme of the connections between the host PC, the positioning sensors, the control hardware, and the linear motors. The input is the target position in the X, Y coordinates, which is entered by the user at the host PC. The control strategy is computed by the PC that receives the position feedback from the laser system. Then, the PC computes the phase voltages that must be

generated for the control hardware to drive the linear motors that produce the movement. The plane mirrors are the moving target of the 2D laser system, and the magnet arrays are the part of the linear motors that perform the relative movement respective to the stator that is fixed. The plane mirrors, as well as the magnet arrays, belong to the moving platform.

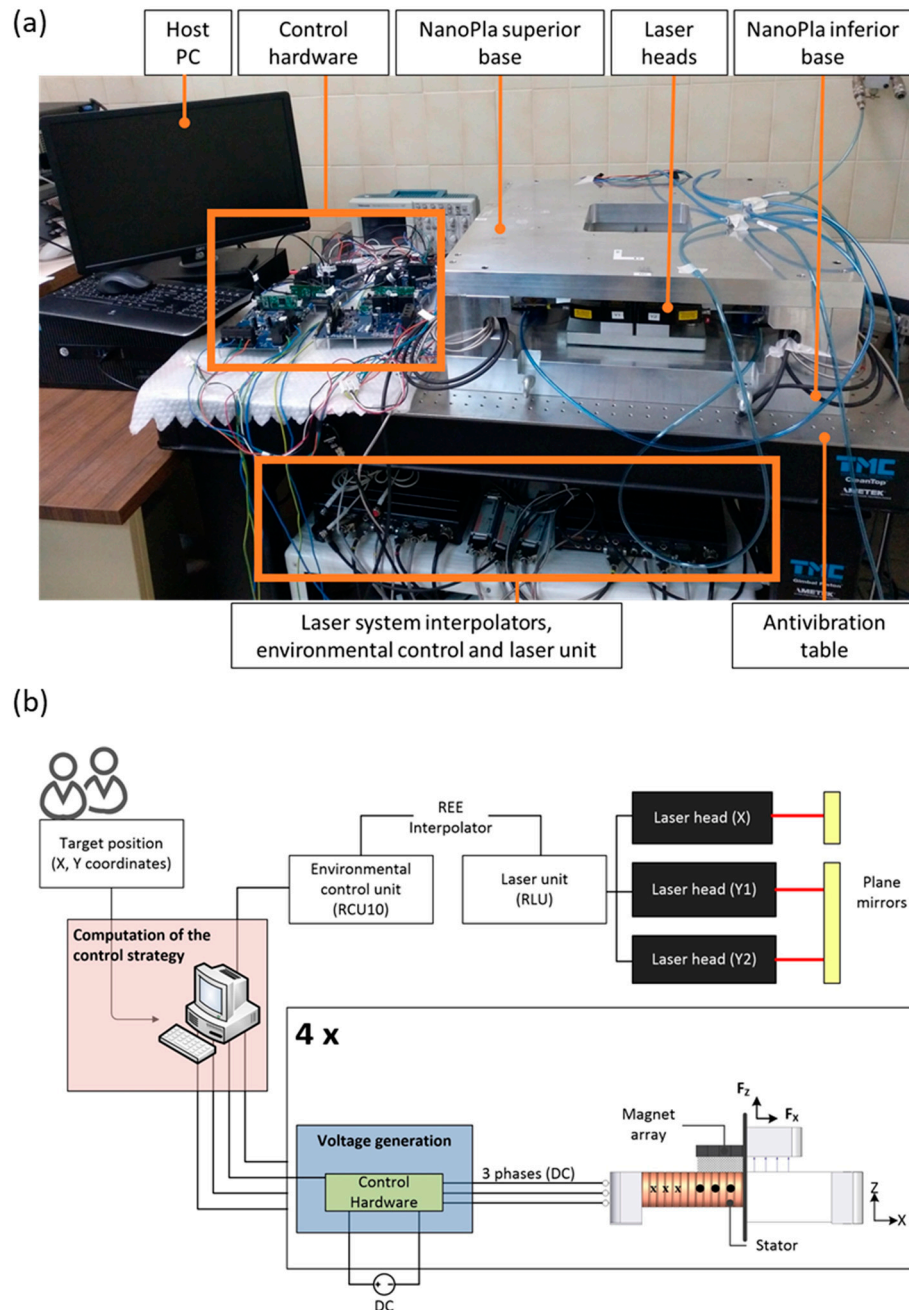


**Figure 2.** (a) Photograph of the NanoPla and the control system components and setup: Host PC, control hardware, and 2D laser system units; (b) scheme of the connections between the host PC, control hardware, and positioning sensor in the 2D positioning control system.

### 3. 2D Positioning Control

After presenting the main components and scheme of the 2D control system, this section first analyses the NanoPla dynamic model and then presents a 2D positioning control strategy for the NanoPla. Finally, the NanoPla’s performance is experimentally validated.



### 3.1. Dynamic Characterisation of the System

In the NanoPla, the motors are placed in parallel pairs (Figure 3); thus, two motors, motor 1 and motor 2 (represented as M1 and M2 in Figure 3b), generate forces on the X-axis ( $F_{M1}$  and  $F_{M2}$ ) that move the platform in the X-direction. Similarly, the other two parallel motors, motor 3 and 4 (M3 and M4), generate forces on the Y-axis ( $F_{M3}$  and  $F_{M4}$ ) that move the platform in the Y-direction. In addition, the four motors are placed symmetrically at a distance R (169.9 mm) from the centre of the platform and, thus, their forces generate a torque at the centre of the moving platform, around the Z-axis. The movements of the platform in the X- and Y-axes  $-X_s$  and  $Y_s$ - and the rotation around Z-axis  $-\theta_{zs}$ - are monitored by the 2D laser interferometer system (Laser Y1, Y2, and X). The total forces in the X- and Y-axes and the torque around the Z-axis  $-T_z$ - can be calculated as follows:

$$F_x = F_{M1} + F_{M2} \tag{1}$$

$$F_y = F_{M3} + F_{M4} \tag{2}$$

$$T_z = -F_{M1} \cdot R + F_{M2} \cdot R - F_{M3} \cdot R + F_{M4} \cdot R \tag{3}$$

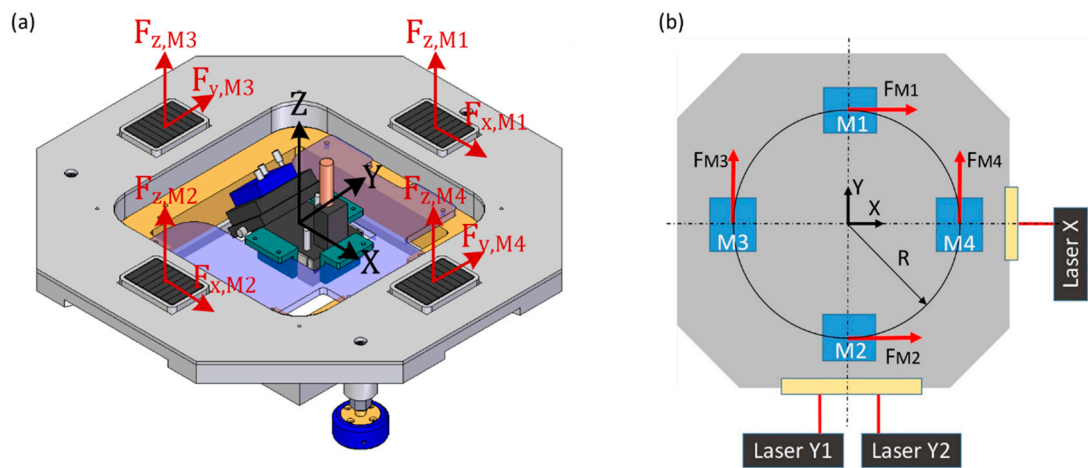


Figure 3. Scheme of the forces that act on the moving platform: (a) isometric view; (b) top view scheme.

The dynamic model of a Halbach linear motor working as a positioning actuator in a pneumatically levitated linear stage was identified as a servosystem in a previous work [14]. In this system, the electromagnetic horizontal force generated by the motor around the stable equilibrium position ( $F_x = 0, F_z > 0$ ) acts as a proportional controller. The closed-loop transfer function that relates the equilibrium position,  $X_{eq}(s)$ , to the position of the stage,  $X(s)$ , was identified with a spring-mass-damper model (second order system). The NanoPla 2D positioning model is expected to present a similar second-order transfer function in each axis of motion, since it uses the same actuators and the moving platform is also pneumatically levitated. The transfer function of the system can be obtained experimentally, which enables a better understanding of the system and allows tuning of the controllers in advance, which facilitates tasks in the experimental setup.

The force generated by each Halbach motor around the stable equilibrium position (linear zone) can be defined as

$$F_{M,x}(s) = K_M(X_{eq}(s) - X(s)) \tag{4}$$

where  $K_M$  is the slope of the thrust force generated by each Halbach linear motor around the equilibrium position. The forces along the X-axis generated by the parallel motor pair M1 and M2 at the initial position are represented in Figure 4. The linear zone and the slope around the stable equilibrium position are also represented in Figure 4. As shown, the linear zone has a length of approximately 5 mm, with the stable equilibrium position in the middle of the region. In this system, the stable equilibrium

position of the parallel pair of Halbach linear motors M1 and M2 is set at the same X-coordinate. Thus, the total force,  $F_x$ , generated around the stable equilibrium position is twice the force defined in Equation (4). Therefore, the transfer function that relates the final position of the stage  $X(s)$  with the defined stable equilibrium position  $X_{eq}(s)$  is the following:

$$\frac{X(s)}{X_{eq}(s)} = \frac{\frac{2K_M}{m}}{s^2 + \frac{b_X}{m}s + \frac{2K_M}{m}} \tag{5}$$

where  $m$  is the mass of the moving part and  $b_X$  defines the viscous-friction elements of the setup and the eddy-current damping of the motors in the X-axis. Additionally,  $2K_M$  is the slope of the total thrust force,  $F_x$ , generated by the pair of Halbach linear motors around the equilibrium position in the X-axis (Figure 4). Since the actuator distribution in the moving platform is symmetrical, the same equations are considered valid for the Y-axis. The mass of the moving platform is known (13.25 kg), and the value of  $K_M$  depends on the reference value set for the vertical force at the stable equilibrium position,  $F_{zref}$ . This value defines the amplitude of the sinusoidal distribution of the forces along the axis of motion, while the spatial period is defined by the design [9]. For instance, when  $F_{zref}$  is set to 1 N,  $K_M$  is approximately 205 N/m, and when  $F_{zref}$  is set to 2 N,  $K_M$  is 410 N/m. Therefore,  $K_M$  and  $m$  are known, whereas the viscous-friction factor  $b_X$  must be obtained experimentally.

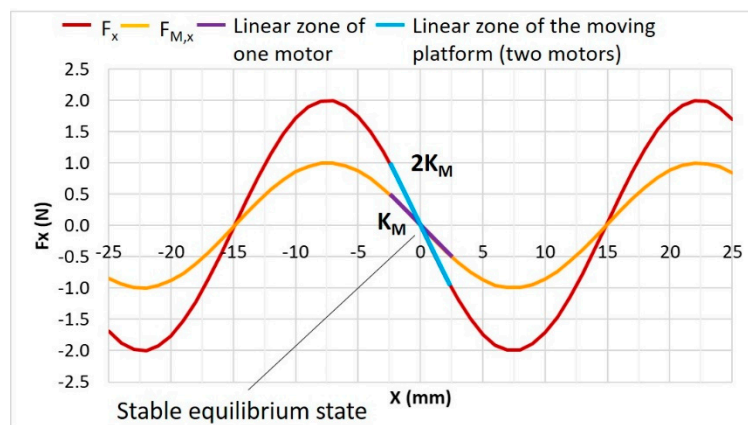


Figure 4. Generated forces by one ( $F_{M,x}$ ) and two motors ( $F_x$ ) along the X-axis of movement.

On the other hand, rotation around the Z-axis ( $\theta_z$ ) is generated by torque acting on the central point of the moving platform. This torque ( $T_z$ ) is the sum of the torques generated by each motor in the plane of motion (Figure 3b). The 2D plane mirror laser interferometer system requires the rotation of the moving platform to be less than  $\pm 1.2 \times 10^{-4}$  rad, according to the manufacturer’s specifications, to prevent misalignment between the laser beam and plane mirror. Therefore, to rotate the moving platform by angle  $\Delta\theta_z$ , each motor would have to perform a displacement of the same magnitude, equal to  $\Delta\theta_z \cdot R$ , in the direction that favours that rotation. According to this, the torque generated by the four motors of the NanoPla to perform a rotation of  $\Delta\theta_z$  can be calculated as follows:

$$T_z = 4K_MR^2\Delta\theta_z \tag{6}$$

It is worth mentioning that the angular position  $\theta_z$  is considered to be a stable equilibrium angular position when, at that angular position, the platform remains still and after a disturbance, it comes back to the same angular position. This stable equilibrium position is created when the moving platform is perfectly aligned in the X- and Y-axes—that is,  $\theta_{z,eq} = 0$ . Thus, as in the previous case, the transfer function that relates the final angular position of the stage  $\theta_z(s)$  with the defined stable equilibrium angular position  $\theta_{z,eq}(s)$  is defined by Equation (7), where  $b_\theta$  is the damping factor in  $\theta_z$ , and  $I_z$  is the inertia of the moving platform.

$$\frac{\theta_z(s)}{\theta_{z,eq}(s)} = \frac{\frac{4K_M R^2}{I_z}}{s^2 + \frac{b_\theta}{I_z} s + \frac{4K_M R^2}{I_z}} \quad (7)$$

### 3.2. 2D Control Strategy

The four motors are placed in parallel pairs. Thus, as long as the motor pairs displace the same distance, the moving platform remains aligned. It was experimentally verified that the moving platform can be positioned along its working range by controlling each of the motors individually with a 1D positioning strategy (presented in [9]) implemented in each motor. Nevertheless, independently controlling each motor results in undesired rotations around the Z-axis during the transient response—that is, when the platform is moving from one position to other. Undesired rotations cause misalignments between the laser beams and plane mirrors, which can affect the performance of the laser system and even impede the displacement measurements. Therefore, in order to prevent undesired rotations of the moving platform during motion, it is necessary to coordinate the control of the four motors in a 2D control strategy.

On the other hand, in [7], control of the out-of-plane motion was proven to be unnecessary due to the high stiffness of the air bearings. Similarly, in the NanoPla, the moving platform is levitated by three vacuum-preloaded air bearings with an input pressure of 0.41 MPa and an input vacuum of 15 mmHg, as recommended by the manufacturer. At these working conditions, the air bearings have a stiffness of 13 N/μm. As calculated in [9], the variation of the vertical force during motion has a maximum increment of 7%, which results in negligible vibrations of the moving platform. Therefore, control of the out-of-plane motion in the NanoPla is unnecessary, although it will be monitored by three capacitive sensors.

The proposed control strategy positions the platform in the X- and Y-axes and minimises rotations around the Z-axis ( $\theta_{z,ref} = 0$ ), to prevent laser system misalignments. This is done with three independent proportional-integral-derivative (PID) controllers that act on the forces generated in the X- and Y-axes by the motor pairs ( $F_x$  and  $F_y$ ) and on the torque ( $T_z$ ) generated by the four motors. The positioning feedback ( $X_s$ ,  $Y_s$ , and  $\theta_s$ ) is provided by the three laser beams (Laser Y1, Y2, and X) of the laser system. Considering the symmetry of the moving platform, the total forces and torque are divided between the four motors, and the horizontal force that each of the motors needs to generate is computed.

Figure 5 illustrates the scheme of the control system that has been implemented in this project. The input of the control system is the target position ( $X_{ref}$ ,  $Y_{ref}$ ) of the moving platform that is entered in the graphic user interface. In addition, the rotation around the Z-axis should be kept minimal ( $\theta_{z,ref} = 0$ ). The previously described control strategy is computed in Simulink® on the host PC (Figure 5). Firstly, this strategy calculates the horizontal forces that each of the linear motors needs to generate to correct positioning errors. Then, the phase currents that each linear motor requires to generate those forces are calculated according to the commutation law defined in [9]. The outputs of the control strategy are the corresponding phase voltages that the control hardware must generate for each motor. These phase voltages are generated at the power stage of each DMC kit. Then, the interaction of the phase currents flowing through the stator coils with the magnetic field of the magnet arrays of the moving platform generates horizontal forces that move the platform. This movement is recorded by the laser system and fed back to the control strategy.



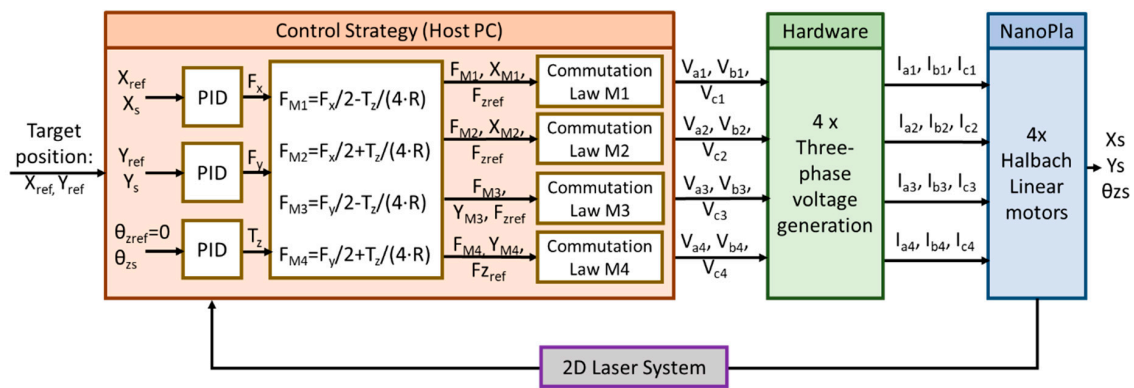


Figure 5. Scheme of the 2D position control system.

### 3.3. Experimental Results

The procedure for experimentally obtaining the transfer function in a linear stage was defined in [14]. This procedure has been adapted to the NanoPla, where a parallel pair (M1 and M2) generates the thrust force in the X-axis, whereas the other parallel pair (M3 and M4) generates the force in the Y-axis (Figure 3). In order to obtain the transfer function in the X-axis, the motor pairs aligned in the Y-axis are set to remain still at the initial position in the Y-axis ( $Y_{ref} = 0, \theta_{z,ref} = 0$ ), acting as a guiding system that prevents the movement of the moving platform on the Y-axis and its rotation around the Z-axis. Then, the NanoPla is displaced from its initial position inside the linear zone by using the electromagnetic force of the motor pair aligned on the X-axis (M1 and M2). The movement of the moving platform is recorded by the laser system, and then the spring mass damper model of Equation (5) is fit to the response. The same procedure is followed to obtain the transfer function on the Y-axis.

Figure 6 represents the experimentally obtained 1 mm step response of the stage on the X- and Y-axes ( $X_s$  and  $Y_s$ ) when  $F_{z,ref}$  is set to 2 N. The simulated response of the adjusted model is also shown ( $X_{sim}$  and  $Y_{sim}$ ). The obtained values for  $m$  and  $K_M$  match the actual mass of the moving platform and the slope of the thrust force around the stable equilibrium position, respectively. The viscous-friction elements ( $b$ ) have a value of 56.8 N·s/m on the X-axis and for 63.07 N·s/m on the Y-axis. The differences between axes could be due to geometrical errors in assembly and the fact that the moving platform is not perfectly symmetrical due to the presence of the plane mirrors, which are larger for the dual beam Y-axis. In addition, it was experimentally verified that by varying  $F_{z,ref}$ , the value of  $K_M$  changed as expected, and the values of  $m$  and  $b$  remained invariable.

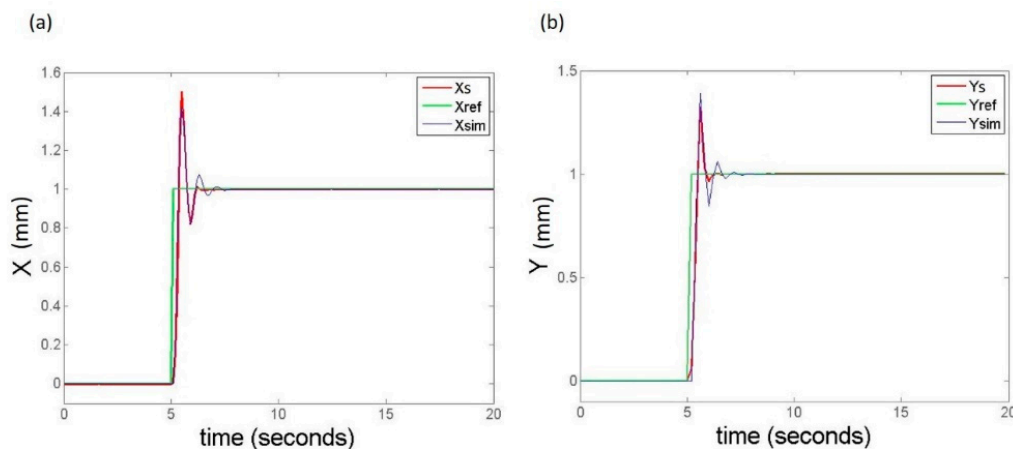
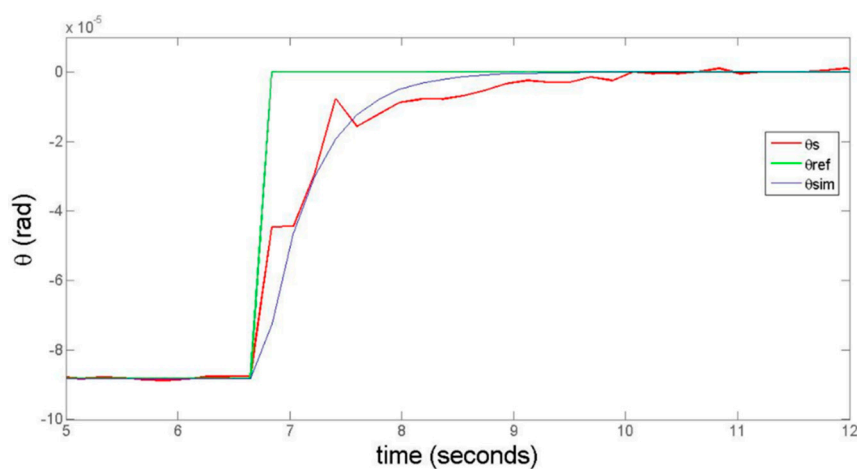


Figure 6. (a) The 1 mm step response on the X-axis of the stage in the open loop and simulation of the plant; (b) the 1 mm step response on the Y-axis of the stage in the open loop and of the simulation of the plant.

In order to obtain the transfer function for the rotation around the Z-axis, the four motors are set to displace from an initial rotated position to a stable equilibrium position  $\theta_{z,eq} = 0$ . At this initial position, the angular deviation is not null. In order to define the initial position, the four motors are displaced at a distance of  $\Delta\theta_z \cdot R$ , equal to  $15 \mu\text{m}$ . In each motor pair, each motor displaces in an opposite direction to contribute to the rotation around the central point of the stage, generating an angular deviation of  $8.83 \times 10^{-5}$  rad, which is close to the maximum displacement allowed without losing the laser system's alignment. The experimentally obtained values for  $I_z$  and  $K_M$  approximately match the actual inertia of the moving platform and the slope of the thrust force around the stable equilibrium position, respectively. Nevertheless, due to the limited range of the angular deviation and the short response time, the recorded response is not smooth enough to perfectly match the simulated plant. Figure 7 represents the experimentally obtained  $8.83 \times 10^{-5}$  rad step response of the stage around the Z-axis ( $\theta_s$ ). The simulated response of the adjusted model is also shown ( $\theta_{sim}$ ).



**Figure 7.** Angular step response of  $8.83 \times 10^{-5}$  rad around the Z-axis of the stage in the open loop and simulation of the plant.

After the transfer function identification, the proposed control system was implemented in the NanoPla, and its correct performance was experimentally verified. For these experiments, the vertical force generated by each motor was defined as 2 N, which limits the phase currents' working range to  $\pm 0.83$  A.

Firstly, the stability of the positioning control system was examined for a long period of time. The moving platform was set to remain still at the initial position for 30 min, and it was experimentally verified that the position deviations are confined to  $\pm 1 \mu\text{m}$ . In Figure 8, a 400 s period of this test is shown, and the root mean square (RMS) deviation during this time is  $0.28 \mu\text{m}$ . The results in the Y-axis are similar, since the moving platform is symmetrical. During this period of time, the force generated by each linear motor varied between  $\pm 2$  mN—that is, the system worked around the stable equilibrium position, as expected.

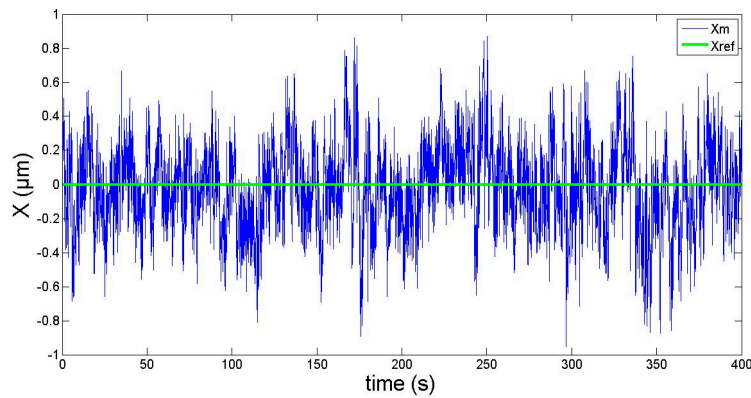


**Figure 8.** Long-term stability analysis of the developed positioning control system.

As mentioned earlier, the NanoPla has a two-stage scheme. The moving platform performs coarse movement in a large working range of 50 mm × 50 mm. Once the moving platform arrives at the target position, it stays static (air bearings off), and a piezo-nanopositioning stage placed on the inferior base performs the fine displacement required for the scanning task. The selected commercial piezostage has a working range of 100 µm × 100 µm in the XY-plane. Therefore, as mentioned, it is defined as a requirement that the position control system has a positioning error smaller than 10 µm, so this error can be corrected by the fine motion of the piezo stage.

Therefore, the performance of the control system was tested when performing a displacement to the target position. Then, 10 µm step responses were taken in the X- and Y-directions. At the same time, the perturbation to the other axis was also recorded, as shown in Figure 9. The perturbed motions in the other axis demonstrate that there is a dynamic coupling between axes. This is unavoidable because there is only one moving part that is affected by the vibrations of the four motors. This perturbation generates a displacement on the Y-axis of a maximum of 2 µm during the transient response. Nevertheless, once the NanoPla achieves its target position on the X-axis, the positioning error on the Y-axis is corrected. In addition, it has been observed that during the transient response, the maximum angular deviation is  $1.5 \times 10^{-5}$  rad, which is inside the tolerance of  $\pm 1.2 \times 10^{-4}$  rad required for the laser system to read.

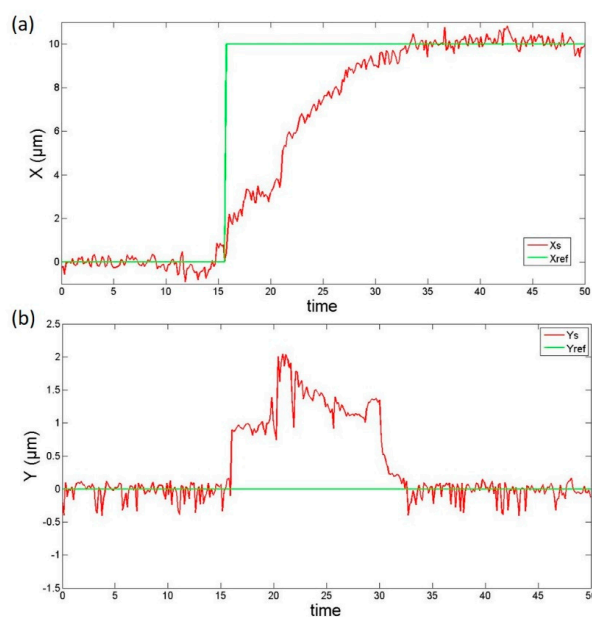


**Figure 9.** The 10 µm step response on the X-axis (a) and perturbation on the Y-axis (b).

Similarly, 100  $\mu\text{m}$  step responses were taken in the X- and Y-directions, while the perturbation to the other axes was also recorded, as shown in Figure 10.

As in the previous case, the displacement in one axis generates perturbations in the other axis. This perturbation generates a displacement of a maximum of 7  $\mu\text{m}$  on the Y-axis during the transient response, which is corrected when the NanoPla achieves its stationary state. In addition, it has been observed that during the transient response, the maximum angular deviation is  $7.3 \times 10^{-5}$  rad, which is inside the tolerance of  $\pm 1.2 \times 10^{-4}$  rad required for the laser system to read.

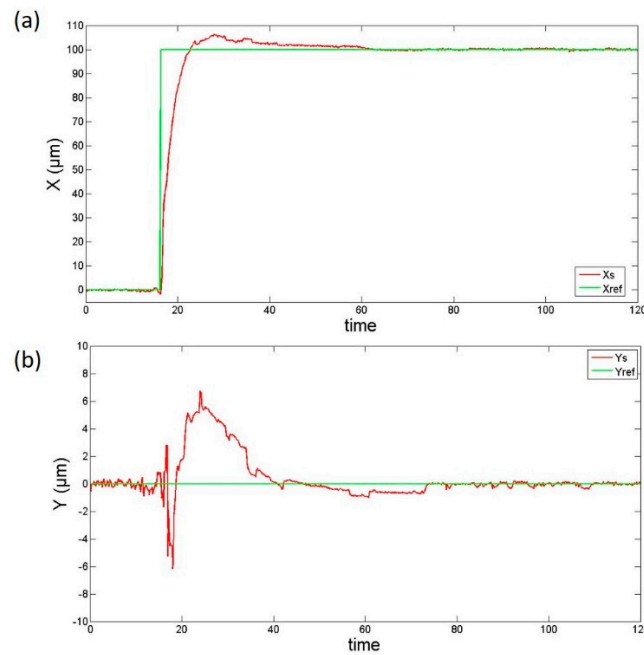


**Figure 10.** The 100  $\mu\text{m}$  step response on the X-axis (a) and the perturbation on the Y-axis (b).

It should be taken into account that the transient response can be adjusted depending on the requirements of the application by changing the parameters of the PID controller.

On the other hand, planar scanning motion is the typical motion used in precision engineering such as nanomanufacturing and metrological characterisation. Several experimental results are presented to demonstrate the scanning capability of the developed positioning control system. Figure 11a shows a displacement on the X-axis of the moving platform from the centre to one extreme of the working range at a constant speed. Similarly, Figure 11b shows a 1 mm forward and backward displacement on the Y-axis.

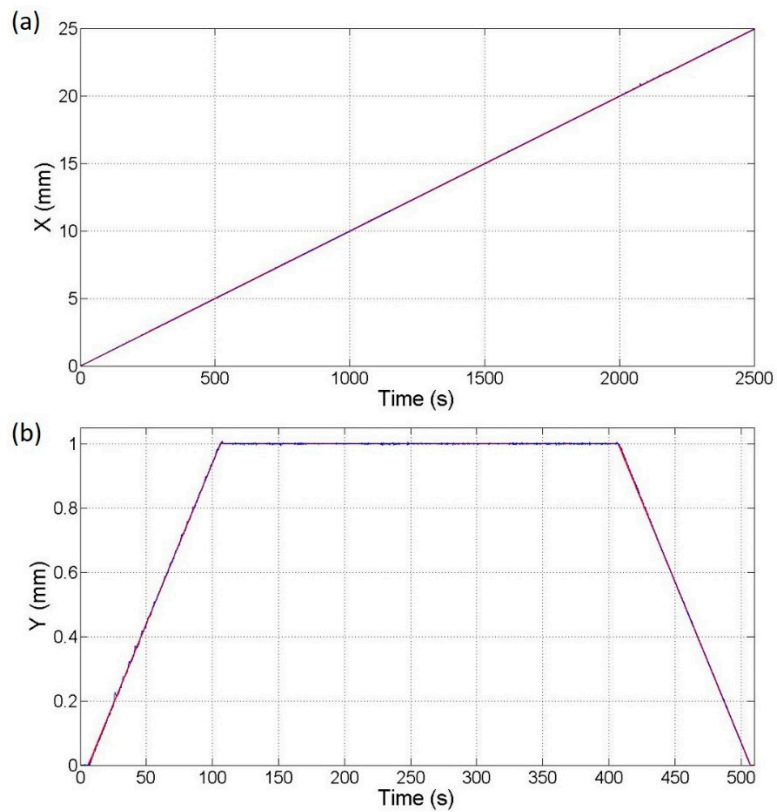


**Figure 11.** (a) The 25 mm displacement at a constant speed on the X-axis; (b) the 1 mm forward and backward displacement at a constant speed on the Y-axis.

In addition, it has been verified that the platform can perform simultaneous movement on the X- and Y-axes without losing the alignment between the laser beam and plane mirrors. Figure 12 illustrates the circular motion performed simultaneously on the X- and Y-axes.

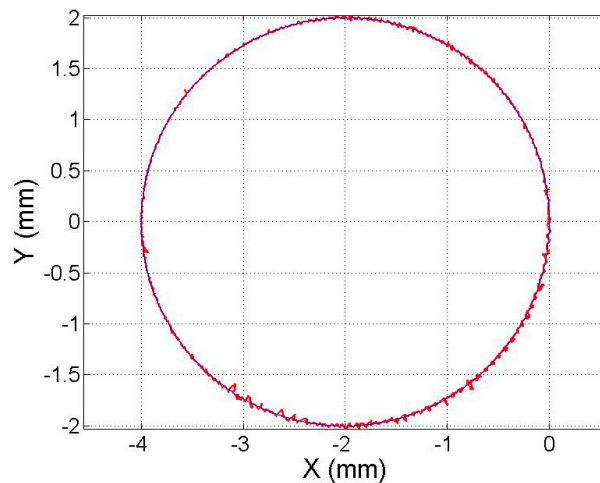


**Figure 12.** Circular motion performed simultaneously on the X- and Y-axes.

#### 4. Positioning Uncertainty of the Control System

The control system of the NanoPla has been optimised to reduce positioning errors. The remaining positioning errors are mainly caused by the resolution of the system components and electronic devices' noise. The computing operation in the control hardware is performed with finite numbers,



which implies a rounding operation, resulting in a truncation error that, depending on its magnitude, may not be negligible. In addition, the errors due to electronic device noise cannot be completely eliminated and result in positioning noise. Thus, the positioning uncertainty of the control system is assessed and analysed in this section.

In Figure 13, the control system dataflow is represented in a block diagram. The data type of the transmitted information is represented by the coloured arrows. The control strategy is computed in Simulink® (MATLAB®).  $X_{ref}$  and  $Y_{ref}$  are the desired positions on the X- and Y-axes. The real position of the NanoPla is measured by a 2D laser system and extracted by MATLAB into the Simulink program. The control strategy computed in the PC by Simulink uses a 64-bit double-precision floating point format (blue arrows), and, in this case, the rounding operation has no significant influence on the calculated results. The control strategy outputs are the required phase voltages, contained in a range of  $\pm 6$  V, and are sent to the control hardware by a serial communication interface (SCI) (green arrows). The MCU of the control hardware works with 32-bit data types, and the voltage values are transmitted as 32-bit fixed points with a 25-bit fraction length (red arrow). The resolution derived from the data type used for the voltages values is 0.0298 nV. These phase voltages are generated in the power stage of the control hardware by PWM. The DMC kit includes a high-resolution PWM (HRPWM) module that is capable of extending the time resolution capabilities of the PWM function. Thus, the resolution of the voltage generation is defined by the time resolution of the HRPWM module and is 26.1  $\mu$ V. This resolution is sufficient to perform a minimum incremental motion of approximately 700 nm in an open-loop. Therefore, this hardware is not able to generate the exact combination of phase currents for every target position. Nevertheless, when working in a closed loop, the positioning controller is capable of partially correcting this error by switching between combinations of phase currents [14].

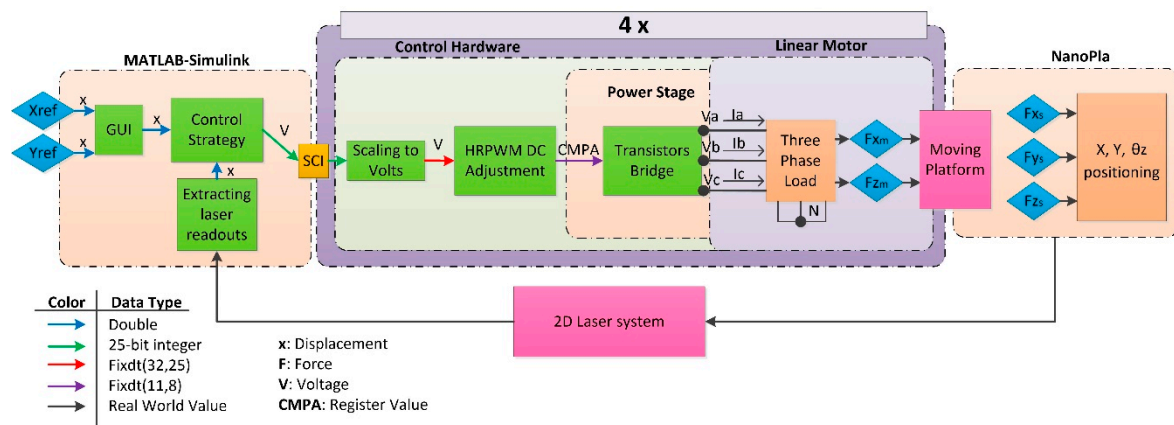
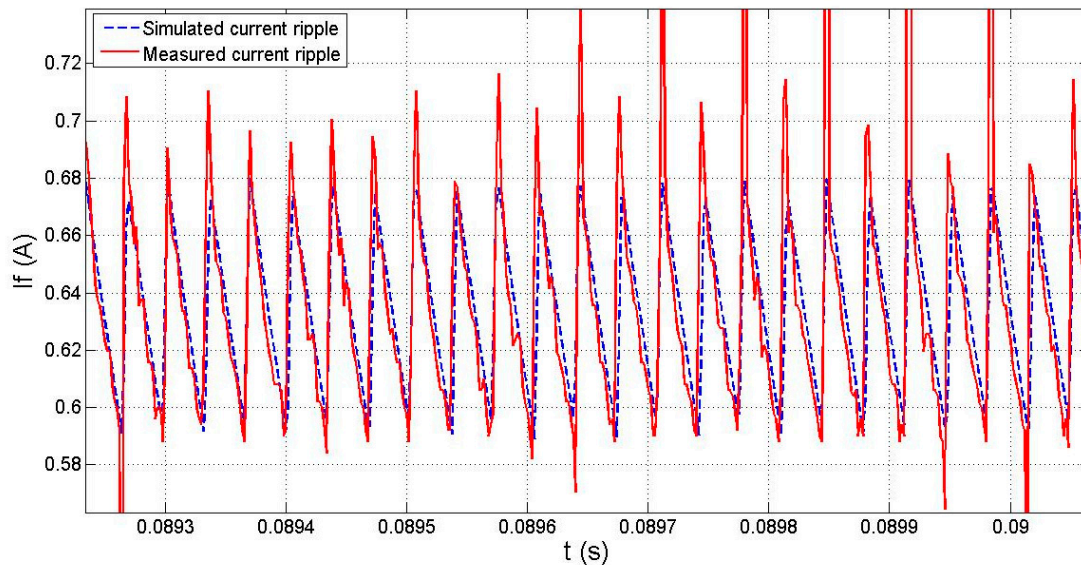


Figure 13. Block diagram of the data flow in the control system of the NanoPla.

In Figure 13, the real-world values are represented with black arrows. These values are the generated phase voltages, the derived currents, and the resultant forces. In addition, the 2D laser interferometer system measures the moving platform’s displacement. The uncertainty of the laser system measurement also affects the positioning uncertainty of the control system.

It must also be taken into account that the PWM-controlled phase voltages lead to a ripple in the phase currents [15]. This current ripple is directly related to the inductance of the stator coils. The resistance and inductance of the coils have been experimentally measured and are 0.88  $\Omega$  and 0.24 mH in each phase coil. The electric circuit has been simulated in order to calculate the current ripple derived from the PWM-generated phase voltages. The current ripple has a sawtooth waveform with a frequency of 29.28 kHz, which is double the PWM frequency. Moreover, the current ripple peak-to-peak value is dependent on the duty cycle (DC) of the PWM voltages; in this study, the current’s working range is  $\pm 0.83$  A, which corresponds to a DC between 43.08% and 56.92%. For these values, the peak-to-peak value of the current ripple has a maximum magnitude of 0.09 A. The actual phase

currents have been experimentally measured using a data acquisition system (DAQ) from National Instruments. This DAQ is able to record the measurements at a frequency of 500 kHz and with a resolution of approximately 2 mA. In Figure 14, an experimentally measured phase current is compared to the simulated one, and, as shown, the current ripple in both cases is almost coincident. Nevertheless, the experimentally measured phase current includes additional noise. This deviation has different sources, including the DAQ's own noise. One of the contributors is the noise of the DC power supply that feeds the power stage of the control hardware. The noise of the DC power supply is imprinted in the PWM phase voltages and, thus, is transmitted to the phase currents. To minimise this contributor, a low-noise power supply, with a peak-to-peak noise of 10 mV, has been used.



**Figure 14.** Current ripple of the phase currents generated by the pulse-width modulation (PWM)-controlled phase voltage.

In a previous study [16], a self-calibration procedure for the geometrical characterization of the 2D laser system of the NanoPla was proposed. The standard uncertainty of the calibrated laser system, after correcting for geometrical errors, was calculated to be 99 nm on the X- and Y-axes. The laser system's resolution is 1.58 nm, and the RMS deviation of the laser readouts of an axis is 6 nm. In addition, the stability of the 2D laser system integrated in the NanoPla was also verified.

In the control system of the NanoPla, the phase current noise generates deviations in the forces that act on the moving platform, thereby producing undesired vibrations in the platform. These vibrations are recorded by the laser system, adding to the laser system's own noise, and fed back to the control strategy. This results in positioning noise of the moving platform that has been experimentally measured and computed as a short term (30 s) RMS positioning error that is 0.11  $\mu\text{m}$  in each axis. It has also been experimentally verified that the main contributor to the RMS positioning error is the phase current's noise.

NanoPla positioning uncertainty contributors can be divided into two categories: Ones whose contribution to the final positioning error in an open loop is known, like the resolution of the phase voltage generation (analysed in [14]) and the laser system (analysed in [16]); and the errors in the laser system that are still present after correcting for the geometrical errors obtained by the self-calibration procedure defined in [16]. The other types of errors are those whose contributions to the final positioning error cannot be calculated separately and cause RMS deviations of the positioning errors. Table 1 illustrates a calculation of the positioning uncertainty according to ISO/TR 230-9:2005 [17] and its contributors. Even though the laser system's resolution is included inside the standard uncertainty of the laser system, its value is also shown separately in the table, so it can be compared to the magnitude of the other contributors.

**Table 1.** NanoPla positioning uncertainty contributors and calculation.

Source	Justification	Standard Uncertainty	Relative Contribution
Resolution at the high-resolution PWM (PWM) $u_{HRPWM}$	Resolution of 26.2 $\mu$ V	0.7/ $\sqrt{12}$ $\mu$ m	65.1%
Laser system resolution $u_{Lres}$	Resolution of 1.58 nm	1.58/ $\sqrt{12}$ nm	0.00%
Laser system calibration $u_{Lcal}$	Geometrical errors + measuring system calibration [16]	99 nm	15.6%
RMS positioning error $u_{RMS}$	Laser system noise + phase currents noise + NanoPla vibrations	0.11 $\mu$ m	19.3%
Positioning uncertainty $U_{XY}(k = 2)$	$U_{XY}(k = 2) = k \sqrt{u_{HRPWM}^2 + u_{Lcal}^2 + u_{Lres}^2 + u_{RMS}^2}$	$\pm 0.50$ $\mu$ m	100%

The resulting positioning uncertainty  $U_{XY} (k = 2)$  in each axis and in the entire working range of 50 mm  $\times$  50 mm is equal to  $\pm 0.50$   $\mu$ m. The main contributor is the HRPWM module resolution, which contributes partially to both. That is, when the laser system detects this error, the controller acts on the horizontal force to correct it, thereby resulting in oscillations. The phase currents' noise is another main contributor to the positioning uncertainty. None of these errors can be corrected without additional electronics. Nevertheless, the resulting positioning uncertainty is much lower than the initial working requirements of the NanoPla, so the developed positioning control system is considered valid.

### 5. Conclusions

In this work, a positioning control system for a 2D nanopositioning stage was designed and implemented in the NanoPla. The proposed control system drives four Halbach linear motors that allow planar motion, while a 2D plane mirror laser interferometer system works as the positioning sensor. The selected control hardware is a Digital Motor Control kit from Texas Instruments for generic three-phase motors. The target is to obtain an accurate positioning control system that fulfils the NanoPla requirements by implementing commercial hardware without any additional electronics.

The NanoPla offers a two-stage scheme that complements the XY-long range positioning of the moving platform (50 mm  $\times$  50 mm) with an additional commercial piezo-nanopositioning stage that is fixed to the inferior base. This second stage works in a range of 100  $\mu$ m  $\times$  100  $\mu$ m. Due to this, the maximum positioning error requirement of the NanoPla in the X- and Y-axes has been decided to be 10  $\mu$ m. In addition, the rotation around the Z-axis must be kept minimal in order to avoid the laser system's misalignment. In this article, a dynamic model for a NanoPla with four Halbach linear motors as actuators was first identified. Then, a control strategy for the positions in the X- and Y-axes and the rotation around Z-axis was designed and implemented for the control hardware. The correct performance of the proposed control system has been experimentally verified for the NanoPla. In addition, the positioning uncertainty of the control system has been computed, and its contributors analysed. The obtained positioning uncertainty  $U_X = U_Y = U_{XY} (k = 2)$  is equal to  $\pm 0.50$   $\mu$ m in each axis and in the entire working range of the NanoPla. Therefore, the resulting positioning uncertainty of the control system implemented in commercial generic hardware without additional electronics is much lower than the initial NanoPla requirements, thus broadening the applicability of the designed positioning system.

In future work, the control strategy could be improved to minimise the coupling between axes during movement. In addition, possible alternatives to improve global uncertainty with additional electronics will be studied. Future research should also focus on the implementation of a measuring system in the NanoPla. As previously noted, the target application of this first prototype is surface topography characterisation at the atomic scale of samples with relatively large planar areas, using an AFM. Nevertheless, due to the fragile configuration of the AFM system, the implementation of a confocal sensor as an intermediate solution before integrating the AFM is proposed.

**Author Contributions:** L.D.-P., M.T., J.A.A., and J.A.Y.-F. developed the positioning control system of the NanoPla.; L.D.-P. performed the experiments and wrote the original draft of the manuscript. M.T., J.A.A., and J.A.Y.-F. reviewed and edited the manuscript.

**Funding:** Funded by the Gobierno de Aragón (Reference Group T56\_17R) and co-funded with Feder 2014–2020 “Construyendo Europa desde Aragón” and the Spanish government project RTI2018-097191-B-I00 “MultiMet” with the collaboration of the Diputación General de Aragón—Fondo Social Europeo.

**Conflicts of Interest:** The authors declare no conflict of interest. The funders had no role in the design of the study; in the collection, analyses, or interpretation of data; in the writing of the manuscript, or in the decision to publish the results.

## References

1. Gao, W.; Kim, S.; Bosse, H.; Haitjema, H.; Chen, Y.; Lu, X.; Knapp, W.; Weckenmann, A.; Estler, W.; Kunzmann, H. Measurement technologies for precision positioning. *CIRP Ann.* **2015**, *64*, 773–796. [[CrossRef](#)]
2. Sato, K. Trend of precision positioning technology. *ABCM Symp. Ser. Mechatron.* **2006**, *2*, 739–750.
3. Manske, E.; Jäger, G.; Hausotte, T.; Füßl, R. Recent developments and challenges of nanopositioning and nanomeasuring technology. *Meas. Sci. Technol.* **2012**, *23*, 74001–74010. [[CrossRef](#)]
4. Torralba, M.; Valenzuela, M.; Yagüe-Fabra, J.; Albajez, J.A.; Aguilar, J.; Fabra, J.A.Y. Large range nanopositioning stage design: A three-layer and two-stage platform. *Measurement* **2016**, *89*, 55–71. [[CrossRef](#)]
5. Trumper, D.; Kim, W.-J.; Williams, M. Design and analysis framework for linear permanent-magnet machines. *IEEE Trans. Ind. Appl.* **1996**, *32*, 371–379. [[CrossRef](#)]
6. Torralba, M.; Yagüe-Fabra, J.A.; Albajez, J.A.; Aguilar, J.J. Design Optimization for the Measurement Accuracy Improvement of a Large Range Nanopositioning Stage. *Sensors* **2016**, *16*, 84. [[CrossRef](#)] [[PubMed](#)]
7. Ruben, S. Modeling, Control, and Real-Time Optimization for a Nano-Precision System. Ph.D. Thesis, University of California, Los Angeles, CA, USA, 2010.
8. Hu, T. Design and Control of a 6-Degree-of-Freedom Levitated Positioner with High Precision. Ph.D. Thesis, Texas A&M University, College Station, TX, USA, 2005.
9. Diaz-Perez, L.C.; Torralba, M.; Albajez, J.A.; Yagüe-Fabra, J.A. One-dimensional control system for a linear motor of a two-dimensional nanopositioning stage using a commercial control hardware. *Micromachines* **2018**, *9*, 421. [[CrossRef](#)] [[PubMed](#)]
10. Diaz-Perez, L.C.; Torralba, M.; Albajez, J.A.; Yagüe-Fabra, J.A. Positioning uncertainty of the control system for the planar motion of a nanopositioning platform. *Procedia Manufacturing*. In Proceedings of the 8th Manufacturing Engineering Society International Conference, Madrid, Spain, 19–21 June 2019.
11. Lu, X.; Usman, I.-U.-R. 6D direct-drive technology for planar motion stages. *CIRP Ann.* **2012**, *61*, 359–362. [[CrossRef](#)]
12. Steinmetz, C. Sub-micron position measurement and control on precision machine tools with laser interferometry. *Precis. Eng.* **1990**, *12*, 12–24. [[CrossRef](#)]
13. Büchner, H.-J.; Jäger, G. A novel plane mirror interferometer without using corner cube reflectors. *Meas. Sci. Technol.* **2006**, *17*, 746–752. [[CrossRef](#)]
14. Díaz-Pérez, L.C.; Albajez, J.A.; Torralba, M.; Yagüe-Fabra, J.A. Vector Control Strategy for Halbach Linear Motor Implemented in a Commercial Control Hardware. *Electronics* **2018**, *7*, 232.
15. Jiang, D.; Wang, F. Current-ripple prediction for three-phase PWM converters. *IEEE Trans. Ind. Appl.* **2014**, *50*, 531–538. [[CrossRef](#)]
16. Torralba, M.; Díaz-Pérez, L.C.; Valenzuela, M.; Albajez, J.A.; Yagüe-Fabra, J.A. Geometrical Characterisation of a 2D Laser System and Calibration of a Cross-Grid Encoder by Means of a Self-Calibration Methodology. *Sensors* **2017**, *17*, 1992. [[CrossRef](#)] [[PubMed](#)]
17. International Organization for Standardization. *ISO/TR 230-9: Test Code for Machine Tools. Estimation of Measurement Uncertainty for Machine Tools Test according to Series ISO 230, Basic Equations*; International Organization for Standardization: Geneva, Switzerland, 2005.



© 2019 by the authors. Licensee MDPI, Basel, Switzerland. This article is an open access article distributed under the terms and conditions of the Creative Commons Attribution (CC BY) license (<http://creativecommons.org/licenses/by/4.0/>).